Journal of Molecular Catalysis A: Chemical 310 (2009) 83–92

Contents lists available at ScienceDirect

Journal of Molecular Catalysis A: Chemical

journal homepage: www.elsevier.com/locate/molcata

Synthesis of titanium–triazine based MCM-41 hybrid materials as catalyst for the asymmetric epoxidation of cinammyl alcohol

Ruth Ballesteros, Mariano Fajardo, Isabel Sierra*, Isabel del Hierro*

Departamento de Química Inorgánica y Analítica, E.S.C.E.T., Universidad Rey Juan Carlos, C/Tulipan S/N, 28933, Móstoles, Madrid, Spain

ARTICLE INFO

Article history:
Received 31 March 2009
Received in revised form 27 May 2009
Accepted 28 May 2009
Available online 6 June 2009

Keywords:
Mesoporous
Titanium
Asymmetric epoxidation

ABSTRACT

A molecular precursor approach involving tethering procedures was used to produce site isolated titanium-supported asymmetric epoxidation catalysts. This was done by first modifying the support in one step with a mixture of silanes: the synthesized triazine propyl triethoxysilane as functional linker and hexamethyldisilizane as capped agent, to increase the hydrophobicity of the support and mask the remaining silanol groups. In addition, $[Ti(OPr^i)_4]$ and $[\{Ti(OPr^i)_3(OMent)\}_2]$ (MentO = 1R,2S,5R-(−)-menthoxo) complexes were heterogenized by reaction with the modified MCM-41. Finally, after $[Ti(OPr^i)_4]$ immobilization on to the organomodified support the reaction with the chiral auxiliary (+)-diethyl-L-tartrate was accomplished. All the materials were characterized by elemental analysis, X-ray diffraction, nitrogen adsorption techniques, FT-IR, ICP-MS, DR-UV–vis, ^{29}Si and ^{13}C MAS NMR and TGA. The different systems were tested in the asymmetric epoxidation of cinnamyl alcohol in order to evaluate their catalytic activity and enantioselectivity.

1. Introduction

Over the last decades, numerous catalytic reactions allowing the formation of enantiomerically pure compounds have been discovered. A family of homogeneous organometallic catalysts using, surprisingly, a small number of ligands, named "privileged structures" [1] show applicability over a wide range of different enantioselective reactions, even on an industrial scale [2]. However, the contribution of asymmetric catalysis to the overall production of chiral chemicals is still low, basically due to the difficulty of recovering the relatively expensive chiral catalyst from the bulk of the reaction. In order to overcome this problem, a great deal of work has been developed to prepare effective heterogeneous catalyst [3,4]. By far, the most widely studied systems are those prepared by immobilization of homogeneous chiral catalyst onto solid supports; by covalent bonding, adsorption, encapsulation, entrapment [5–7], etc. and lately, by sol–gel hydrolysis condensation of silylated chiral ligands or silylated chiral complexes [8,9]. The support must be thermally, chemically, and mechanically stable during the reaction process and its structure must make possible the good dispersion of the active sites, which must be also easily accessible. Organic–inorganic hybrid materials meet these criteria by exploiting the physical robustness of porous inorganic materials and the chemical functionality of organic materials. Among them, mesoporous type materials grow in importance as a result of their regular structures and tuneable pore diameters. In addition, increased activity and selectivity can also be observed upon immobilization in a confined space, due to the confinement effect originated from the weak interactions between catalyst/substrate and pore surfaces. Therefore, the enantioselectivity can be improved by careful tuning the confinement effect based on the molecular designing of the pore/surface and the immobilized catalysts according to the requirements of chiral reactions [10].

Sharpless asymmetric epoxidation of allylic alcohols has become a highlight classic in asymmetric catalysis. In this process, well understood by now, the chiral ligand plays a critical role in the enantioselectivity. The catalytically active species is titanium dimer, containing two dialkyl tartrate ligands and both the oxidant and the allylic alcohol coordinated. Nevertheless, there are few reports on the assemblies of chiral titanium complexes over solid supports in order to achieve the heterogenization of these catalyst components. Nearly two decades ago, Choudary et al. [11] carried out the immobilization of a heterogeneous chiral titanium catalyst on an inorganic support, a combination of dialkyl tartrate and titanium-pillared montmorillonite resulted in excellent ee in the epoxidation reaction of several allylic alcohols ranging from 90% to 98%. Johnson and co-workers [12] published a variety of Ti (IV) complexes, as molecular models of heterogeneous silica based systems, in which the titanium was coordinated to only one or two siloxides of a partially silylated silsesquioxane backbone in order to modify the degree of steric congestion around the titanium (IV) active site. These new complexes were performed in their chiral

* Corresponding author. Tel.: +34 914887022; fax: +34 914888143.
E-mail address: isabel.hierro@urjc.es (I. del Hierro).

1381-1169/$ – see front matter © 2009 Elsevier B.V. All rights reserved.
doi:10.1016/j.molcata.2009.05.023

version by reaction with BINOL but they resulted inactive epoxidation catalysts. Basset and co-workers [13] reported silica-supported tantalum catalysts for the enantioselective epoxidation of allylic alcohols in the presence of chiral tartrate derivatives with comparable results to that obtained in the homogeneous Sharpless reaction, however, the tantalum precursors were not easy to prepare. Some years later, Fu et al. [14] reported the grafting of titanium tartrate complexes onto HMS by reaction of TiL_4 (L = OPr^i, Cl) and D-tartaric acid with the surface OH groups. Recently, our group has reported the grafting of $[\{Ti(OPr^i)_3(OMent)\}_2]$ and $[Ti(OMent)_4]$ to prepared SBA-15 based catalyst rendering medium yields and low ee. Interestingly, the chiral induction obtained was the contrary to those of the analogous homogeneous systems and similar to that prompted by the silsesquioxane complex modelling the heterogeneous systems [15]. A different strategy was followed by Li and co-workers, who grafted a chiral tartaric acid onto the surface of silica and in the mesoporous of MCM-41 providing and effective heterogeneous catalyst for asymmetric epoxidation of allylic alcohols by further reaction with $Ti(OPr^i)_4$ [16].

The main objective in this study is to obtain well-defined organotitanium compounds tethered onto capped MCM-41 capable of acting as active catalyst in the Sharpless epoxidation process, in the presence of a chiral auxiliar or, in a parallel way, the synthesis of well-defined tethered organotitanium compounds in which the chiral moiety is kept bonded to titanium.

2. Experimental procedure

2.1. General remarks

All reactions were performed using standard Schlenk tube techniques under an atmosphere of dry nitrogen or argon.

2.2. Reagents and materials

Sulphuric acid 98% (M = 98.08, d = 1.840 g mL^{-1}) was purchased from Panreac. Sodium silicate SiO_2·NaOH (M = 242.23, d = 1.390 g mL^{-1}), cetyltrimethylammonium bromide (CTAB) (M = 364.46), hexamethyldisilazane (HMDS) and 1R,2S,5R-(−)-menthol were purchased from Sigma–Aldrich and used as supplied. Titanium tetraisopropoxide $Ti(OPr^i)_4$ (0.955 g mL^{-1}, 97%) was purchased from Sigma–Aldrich distilled and stored under an argon atmosphere prior to use. Cinnamyl alcohol, (+)-diethyl-L-tartrate (L-DET) and tertbutylhydroperoxide (TBHP) (5–6 M decane) were purchased from Sigma–Aldrich and stored in presence of molecular sieves. Organic solvents (toluene and dichloromethane) were purchased from SDS, distilled and dried before use according to conventional literature methods. Triazine propyl triethoxysilane ligand (CyPTS) and the modified MCM-41 (CyPTS-HMDS-MCM-41) were prepared by previously reported procedure [17]. Synthesis and characterization of $[\{Ti(OiPr)_3(OMent)\}_2]$ was also reported by our group [18].

2.3. Synthesis of MCM-41 mesoporous silica

A hexagonal (plane group p6mm) material (MCM-41) was prepared according to the method of Landau et al. [19] using hydrothermal crystallization. A sodium silicate solution (65.45 g, 14% NaOH; 27% SiO_2) was mixed with 4.20 g of 98% sulphuric acid and 140 mL of water. The mixture was stirred for 30 min at room temperature. Cetyltrimethylammonium bromide (58.66 g) dissolved in 176 mL of water was added. The resulting gel was mixed with 70 mL of water (stirred at room temperature for 30 min). The gel was transferred to a Teflon-coated autoclave and heated at 121 °C for 144 h. A solid was produced, separated by suction filtration and dried at 100 °C for 8 h. The surfactant was removed by calcination in air at 530 °C for 6 h.

2.4. Preparation of titanium modified MCM-41-supported catalyst

2.4.1. Preparation of Ti-CyPTS-HMDS-MCM-41 and TiMent-CyPTS-HMDS-MCM-41

The titanium containing mesoporous materials were prepared by reaction of $Ti(OPr^i)_4$ or $[\{Ti(OPr^i)_3(OMent)\}_2]$ with the chemically modified MCM-41 silica (CyPTS-HMDS-MCM-41). In a typical experiment $[\{Ti(OiPr)_3(OMent)\}_2]$ or $Ti(OPr^i)_4$ (4 mmol) was added to 4 g of the organomodified silica suspended in dry toluene and stirred for 24 h in order to obtain TiMent-CyPTS-HMDS-MCM-41 and Ti-CyPTS-HMDS-MCM-41 catalysts, respectively. The solid was filtered off, washed repeatedly with toluene and dried under vacuum in order to remove the volatiles.

Ti-CyPTS-HMDS-MCM-41: ^{13}C CP/MAS NMR δ = −6 (≡Si–O–Si(***C***H_3)$_3$), 9 (O–CH_2–CH_2–***C***H_2–Si), 18 (Si(OCH_2***C***H_3)), 21.5 (O–CH_2–***C***H_2–CH_2–Si), 25 (Ti–O–CH(***C***H_3)$_2$), 40.5 (O–***C***H_2–CH_2–CH_2–Si), 58 (Si(O***C***$H_2$$CH_3$)), 68 (Ti–O–***C***H($CH_3$)$_2$), 150 (N–***C***–OH (***C***$_3N_3$)).

TiMent-CyPTS-HMDS-MCM-41: ^{13}C CP/MAS NMR δ = −2.5 (≡Si–O–Si(***C***H_3)$_3$), 11 (O–CH_2–CH_2–***C***H_2–Si), 17 (Si(OCH_2***C***H_3)), 21.5 (O–CH_2–***C***H_2–CH_2–Si), 21.5 (Ti–O–CH(***C***H_3)$_2$), 40.5 (O–***C***H_2–CH_2–CH_2–Si), 58 (Si(O***C***$H_2$$CH_3$)), 68 (Ti–O–***C***H($CH_3$)$_2$), 146 (N–***C***–OH (***C***$_3N_3$)).

Ti-menthoxo unit	
C1	84
C2	53.3
C3	21.5 (C_9 + C_7 + C_3)
C4	32.5 (C_4 + C_5)
C5	32.5 (C_4 + C_5)
C6	46.1
C7	21.5 (C_9 + C_7 + C_3)
C8	28
C9	21.5 (C_9 + C_7 + C_3)
C10	14

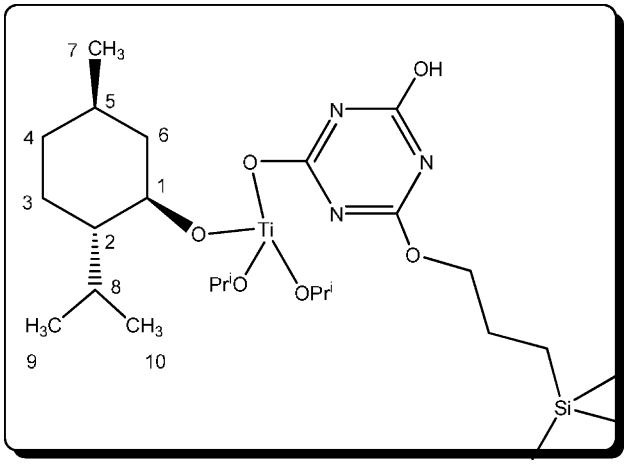

2.4.2. Reaction of Ti-CyPTS-HMDS-MCM-41 and L-(+)-DET

In a typical experiment, (+)-diethyl-L-tartrate (0.22 mL, 1.35 mmol) was added to 1 g of Ti-CyPTS-HMDS-MCM-41 previously suspended in dichloromethane. The mixture was stirring at room temperature during 24 h.

^{13}C CP/MAS NMR $\delta = -0.10$ (≡Si–O–Si(***C***H_3)$_3$), 9 (O–CH_2–CH_2–***C***H_2–Si), 18 (Si(OCH_2***C***H_3)), 18 (CO–O–CH_2***C***H_3)), 23 (O–CH_2–***C***H_2–CH_2–Si), 23 (Ti–O–CH(***C***H_3)$_2$), 43 (O–***C***H_2–CH_2–CH_2–Si), 59 (Si(O***C***H_2CH_3)), 59 (CO–O–***C***H_2CH_3)), 68 (Ti–O–***C***H(CH_3)$_2$), 85 (Ti–O–***C***–$CO_2CH_2CH_3$), 149 (N–***C***–OH (***C***$_3N_3$)), 170.8 (***C***O–O–CH_2CH_3).

2.5. Catalytic test

A flame dried 250 mL two-necked flask was fitted with a dropping funnel, flushed with nitrogen and charged with 1 g of activated, powdered 4 Å molecular sieves, 0.25 g of the tested catalyst and 50 mL of dry CH_2Cl_2. The mixture was cooled to −20 °C and t-Bu^{t}OOH in decane was added. The mixture was allowed to stir at −20 °C for 1 h and then treated with freshly distilled (E)-3-phenyl-2-propenol (cinnamyl alcohol) in CH_2Cl_2 (0.1 M), added drop wise over 1 h. The resulting mixture was stirred 12 h to −20 °C. The solid was recovered from the solution by filtration and washed several times with CH_2Cl_2. The volatiles were removed under vacuum to get yellow oil. ^1H NMR (400 MHz, $CDCl_3$, 25 °C): $\delta = 2.15$ (brs, 1 H, –OH), 3.22–3.25 (m, 1 H, –C*H*–CH_2), 3.81 (dd, 1 H, –CH_2), 3.94 (d, 1 H, Ph–C*H*), 4.06 (dd, 1 H, –CH_2), 7.2–7.4 (m, 5 H, C_6H_5). The yields and enantiomeric excess values of the so obtained epoxy alcohols were determined by HPLC with a chiralpak AD-H column from VWR International Eurolab [20]. In order to reuse the catalyst the solid was then washed with dichloromethane, in order to remove any organic species remaining adsorbed, dried and tested again under similar experimental conditions.

2.6. Characterization

X-ray diffraction (XRD) patterns of the silicas were obtained on a Phillips Diffractometer model PW3040/00 X'Pert MPD/MRD at 45 kV and 40 mA, using Cu Kα radiation (λ = 1.5418 Å). N_2 gas adsorption–desorption isotherms were obtained using a Micromeritics TriStar 3000 analyzer, and pore size distributions were calculated using the Barret–Joyner–Halenda (BJH) model on the adsorption branch. Infrared spectra were recorded on a Nicolet-550 FT-IR spectrophotometer in the region 4000–400 cm^{-1}) as KBr disks. ^1H NMR spectra were recorded on Varian FT-300 and Varian FT-400 spectrometers and chemical shifts were measured relative to residual ^1H and ^{13}C resonances in the deuterated solvents Proton-decoupled ^{29}Si MAS NMR spectra were recorded on a Varian-Infinity Plus 400 MHz Spectrometer operating at 79.44 MHz proton frequency (4 μs 90° pulse, 1024 transients, spinning speed of 5 MHz). Cross Polarization ^{13}C CP/MAS NMR spectra were recorded on a Varian-Infinity Plus 400 MHz Spectrometer operating at 100.52 MHz proton frequency (4 μs 90° pulse, 4000 transients, spinning speed of 6 MHz, contact time 3 ms, pulse delay 1.5 s). Elemental analysis (%C and %N) was performed by the Investigation Service of the Universidad de Alcalá de Henares de Madrid (Spain) using a CHNS analyser LECO-932 model. The thermal stabilities of the modified mesoporous silicas were studied using a Setsys 18 A (Setaram) thermogravimetric analyzer. The DR UV–vis spectroscopic measurements were carried out on a Varian Cary-500 spectrophotometer equipped with an integrating sphere and PTFE (Polytetrafluoroethylene) as reference, with $d = 1$ g/cm^3 and thickness of 6 mm. The titanium content was determined by ICP-atomic emission spectroscopy (ICP-AES) using a Varian Vista AX model. The samples (0.1 g) were dissolved in aqueous hydrofluoric and sulphuric acid. After dissolution, the sample was heated to evaporated water and hydrofluoric acid and the sample was transferred into 250 mL calibrated flask and diluted with water. An absorption standard solution of Ti (1000 μg/mL in water) was used for the calibration of the equipment. HPLC analyses were performed on a Varian chromatographic system containing a 210/215 ProStar pump, a manual injection valve Rheodyne model 7752i equipped with a 20 μl sample loop, a 320 ProStar UV-vis detector and a personal computer-based data acquisition system Star Chromatography Workstation version 5. The chromatographic separations were performed, using a chiralpak AD [amylase tris(3,5-dimethylphenylcarbamate) coated on silicagel, 250 mm × 4.6 mm i.i.; 10 μm particle diameter] column (Chiral technologies Europe, Illkirch, France) at ambient temperature.

3. Results and discussion

3.1. Synthesis and characterization of heterogeneous catalysts

One of the challenges that offer the widespread used titanium alkoxo complexes is the difference between the structures in solid state and in solution, where mixtures of monomers, dimers and so on, may coexist due to association equilibrium. Such structural richness ensures flexibility and efficiency of this type of titanium catalysts but make difficult to transfer the information relative to the solid state structure of the catalyst to the solution where the majority of reactions takes place [21]. Here, we report the preparation of new heterogeneous catalysts by reaction of titanium alkoxo derivatives with the previously functionalized MCM-41 support with a mixture of silanes. Firstly, the triazine based ligand which acts as a polydentate alcohol providing a rigid framework for the metal centre and might serve to control the oligomeric nature of metal alkoxides [22]. Secondly, the disilazane reagent HN($SiMe_3$)$_2$ (HMDS), which allows the conversion of the remaining hydroxyls on to the silica surface into trimethylsilyl groups (Me_3Si–O–Si≡) increasing the hydrophobic character of the materials and avoiding the presence of the acid OH groups, incompatible with the catalytic reaction under study. In addition, the presence of two hydroxyl units in the triazine ligand brings up the possibility of coordination of at least two metal centres by attached ligand and may control the titanium loading on to the support [23].

To prepare the grafted titanium complexes, titanium tetraisopropoxide, Ti(OPr^i)$_4$ or [{Ti(OPr^i)$_3$(OMent)}$_2$] (MentO = 1R,2S,5R-(−)-menthoxo) were dissolved in toluene and added to a suspension of the functionalized mesoporous silica (Scheme 1). The reaction was maintained 24 h under stirring; the solids were recovered by filtration and washed intensively with toluene. In this way, Ti-CyPTS-HMDS-MCM-41 and TiMent-CyPTS-HMDS-MCM-41 were obtained (Scheme 1).

From elemental analysis the CyPTS ligand loading was found to be 0.80 mmol g^{-1} for CyPTS-HMDS-MCM-41 on the basis of nitrogen content measurements (Table 1). The amount of capped ligand was estimated according to the carbon content and loading of CyPTS ligand, to be 2.72 mmol g^{-1} of HMDS. The amount of titanium determined by ICP-AES was 0.79 and 0.70 mmol g^{-1} for Ti-CyPTS-HMDS-MCM-41 and TiMent-CyPTS-HMDS-MCM-41, respectively. Taking into account the ligand loading, the Ti/CyPTS ratio suggested the formation of complexes with 1:1 stoichoimetry. The observed titanium loading values for the grafted samples were comparable with other materials previously prepared by Tilley et al. by using [(OBu^t)$_2$Ti{μ-O_2Si(OSi(OBu^t)$_3$]$_2$})$_2$] [24], [Ti{OSi(OBu^t)$_3$}$_4$], [(OPr^i)Ti{OSi(OBu^t)$_3$}$_3$] and [(OBu^t)$_3$Ti{OSi(OBu^t)$_3$}] [25] as precursors and by our own group by using [{Ti(OPr^i)$_3$(OMent)}$_2$] and [Ti(OMent)$_4$] titanium alkoxo complexes bearing menthoxo units.

To gain insight into the chemistry of the grafting process, solution ^1H NMR spectroscopy was used to monitor the grafting chemistry of [{Ti(OPr^i)$_3$(OMent)}$_2$] onto the silica surface.

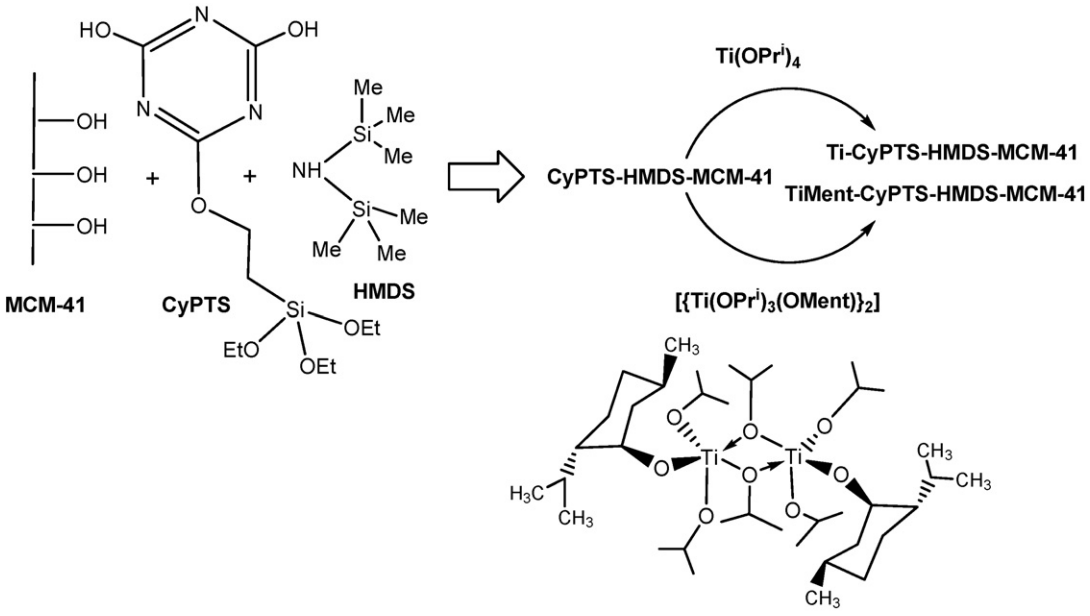

Scheme 1.

The reaction of CyPTS-HMDS-MCM-41 with a solution of a large excess of [{Ti(OPr^i)$_3$(OMent)}$_2$] should result in the elimination of isopropanol or menthol. The elimination products were indeed identified to be both Pr^{i}OH and MentOH with an integral ratio 3.5:1 after 48 h reaction in toluene at 100 °C. This result was in agreement with the formation of titanium complexes bearing preferently a chiral moiety.

The mesostructures of complex immobilized materials were confirmed by X-ray diffraction and nitrogen adsorption–desorption techniques. Unmodified MCM-41 display a well-resolved pattern at low 2θ values with a very sharp (1 0 0) diffraction peak at 2.49 and three additional high order peaks (1 1 0), (2 0 0) and (2 2 0) with lower intensities indicating the well-developed mesopore structure, d-spacing value for this XRD peak was 35.48 Å and a_0 was equal to 40.97 Å. As can be seen in Fig. 1 a well-resolved pattern, with a significant peak, was obtained for the rest of samples indicating a good mesoscopic order. Compared to parent MCM-41 the titanium tethered triazine propyl samples show a decrease in the d-spacing and a significant attenuation of the XRD peak intensities. This latter is not interpreted as a loss of crystallinity. Instead, it is likely that there is a reduction in the X-ray scattering contrast between the silica framework and the metal–organic moieties which are located inside the channels of the host.

The textural properties such as specific surface area (S_{BET}, $m^2\,g^{-1}$) and pore volume ($cm^3\,g^{-1}$) of the support were followed throughout the different modification processes. For the parent MCM-41 system and functionalized materials the isotherms are type IV according to the IUPAC classification and have an H1 hysteresis loop that is representative of mesoporous cylindrical or rod-like pores (Fig. 2). The volume adsorbed for all isotherms increased sharply at a relative pressure (P/P_0) of 0.4, which represents capillary condensation of nitrogen within the uniform mesoporous structure. The inflection position shifted slightly to lower relative pressures and the volume of nitrogen adsorbed decrease upon silylation and titanium incorporation, which is indicative of a reduction in the pore size. The physical parameters of the nitrogen isotherms, such S_{BET}, pore volume and BJH average pore diameter, for mesoporous silicas are shown in Table 2. The MCM-41 material posses high S_{BET} (993 m^2/g) and a BJH pore diameter of 28.5 Å, these values are typical of surfactant-assembled mesostructures. The wall thickness for MCM-41 (12.47 Å) was calculated as ($2d_{100}/\sqrt{3}$-BJH pore diameter). After silylation and titanium incorporation a decrease in the S_{BET}, pore volume and average BJH pore diameter were observed, changes that can be interpreted as being due to the presence of organotitanium molecules anchored to the channels partially blocking the adsorption of nitrogen molecules. The average pore diameter clearly decreases after the incorporation of titanium isopropoxo species by reaction with the organofunctionalized mesoporous silica. In this way the sample TiMent-CyPTS-HMDS-MCM-41 with the more sterically demanding groups exhibits a higher decrease in the surface area and pore volume, as well as, an increase in the wall thickness. The narrow pore size distribution found for Ti-CyPTS-HMDS-MCM-41 and

Table 1
Ligand and titanium loading of MCM-41 functionalized material.

Catalyst	%C[a]	%N[a]	CyPTS/mmol g^{-1}	Ti[b]/mmol g^{-1}
Ti-CyPTS-HMDS-MCM-41	14.94	3.37	0.80	0.79
TiMent-CyPTS-HMDS-MCM-41	26.70	3.33	0.80	0.70

Molar surface loading of CyPTS = mmol g^{-1} N/3.
[a] From elemental analysis.
[b] From ICP-AES.

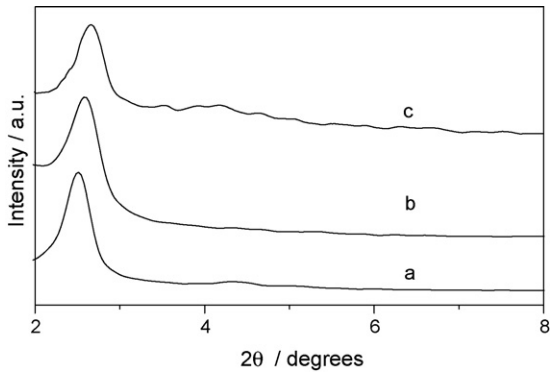

Fig. 1. Powder X-ray diffraction patterns of (a) MCM-41, (b) Ti-CyPTS-HMDS-MCM-41 and (c) TiMent-CyPTS-MTMS-MCM-41.

Table 2
Textural properties of the mesoporous MCM-41 materials.

Catalyst	S_{bet} ($m^2\,g^{-1}$)	Pore volume (cm^3g^{-1})	Pore diameter (Å)	d_{100} (Å)	a_0 (Å)	Wall thickness (Å)
MCM-41	993	0.71	28.5	35.5	41.0	12.5
Ti-CyPTS-HMDS-MCM-41	508	0.28	18.5	34.4	39.8	21.3
TiMent-CyPTS-HMDS-MCM-41	246	0.12	14.1	33.6	38.7	24.6

TiMent-CyPTS-HMDS-MCM-41 (centred at 15.7 and 9.2 Å) provides evidence for its uniform framework mesoporosity and confirms the reduction of the pore sizes after the modification process. From the TEM micrographs (as shown in Fig. 3), we could find that the ordered pore structure was still preserved after modification treatment processes

FT-IR spectra of pure MCM-41, Ti-CyPTS-HMDS-MCM-41 and TiMent-CyPTS-HMDS-MCM-41 between 4000 and 400 cm^{-1} are reported in Fig. 4. The main features of the MCM-41 spectra include a large broad band between 3400 and 3200 cm^{-1}, which is attributed to O–H stretching of the surface silanol groups and the remaining adsorbed water molecules. The siloxane (–Si–O–Si–) band appears as a broad strong peak centred at 1100 cm^{-1}. The band due to Si–O bond stretching of the silanol groups was observed at 960 cm^{-1}. The adsorption band at 1630 cm^{-1} is due to deformation vibrations of adsorbed water molecules [26]. The Ti containing materials show characteristic bands for aliphatic C–H stretching vibrations due to $Me_3Si–O–Si\equiv$, silane–triazine ligand, menthoxo and isopropoxo groups around 2900 cm^{-1}. Other prominent features of the IR spectra, for the samples with the triazine ligand, are the bands observed at 1475 and 1720 cm^{-1} assigned to the aromatic ring and C=N stretching vibration, respectively. The bands typical of menthoxo groups appear at 2964 cm^{-1} ($\nu_{as}(CH_3)$), 2923 cm^{-1} ($\nu_{as}(CH_2)$), 2883 cm^{-1} ($\nu_s(CH_3)$), 2851 cm^{-1} ($\nu_s(CH_2)$), 1420 and 1405 cm^{-1} ($\delta_a(CH_2)$, $\delta_a(CH_3)$), and 1366 cm^{-1} $\delta_s(CH_3)$, the two last bands are characteristics of isopropyl groups. The absorption peak at 657 and 532 cm^{-1} are assigned to Ti–O–C bonds.

The ^{29}Si MAS-NMR spectra in the solid state for parent MCM-41 and functionalized silicas confirm the covalent bond formed between the silylating agents CyPTS and HMDS and the silanol groups dispersed on the surface (see Fig. 5). Unmodified silica (Fig. 4a) shows two main peaks at −110 and −98 ppm assigned to Q^4 framework silica sites ($(SiO)_4Si$) and Q^3 silanol sites ($(SiO)_3SiOH$), respectively. A weak resonance is also present at about −92 ppm corresponding to the Q^2 species ($(SiO)_2Si(OH)_2$). Q^4 is clearly the dominant peak in both spectra because it is the most abundant site. The spectra of the functionalized silica show a marked decrease in the intensity of the Q^3 signal, which verified the tethering of the functional groups to Si–OH. T^2 ($RSi(OSi)_2(OR')$) and T^3 ($RSi(OSi)_3$) organosilane species at −55 and −67 ppm, respectively, present in the CyPTS functionalized materials are indicative of a high degree of condensation of the triethoxysilanes with the silica surface. In addition, the choice of HMDS as protecting group allows an easy determination of the trimethylsilyl groups by ^{29}Si NMR; the new peak of the silylating agent, an M site ($(Me_3SiO–$), is seen at 12 ppm.

Titanium containing materials have been also characterized with ^{13}C CP-MAS NMR (Fig. 6). For Ti-CyPTS-HMDS-MCM-41 the signals from the three carbon atoms present in the alkyl chain of the bound linker appears at 10, 21 and 40.5 ppm for $\equiv Si–\boldsymbol{C}H_2–$, $CH_2–\boldsymbol{C}H_2–CH_2–$ and $–\boldsymbol{C}H_2–O$, respectively. The aromatic carbons $\boldsymbol{C}_3N_3$ of triazine ring appears at 145 ppm and two signals at 25 and 68 ppm are attributed to methyl $(\boldsymbol{C}H_3)_2–CH–O$ and methyne $(CH_3)_2–\boldsymbol{C}H–O$ groups of the isopropoxo ligands attached to titanium. In addition two additional signals at 18 and 58 ppm attributed to the unreacted ethoxo groups attached to Si in the triazine silane ligand are observed. Finally, at −6 ppm appears a signal due to the trimethylsilyl carbon atoms $(\boldsymbol{C}H_3)_3Si–O–Si\equiv$ of the silylating agent. The analysis of ^{13}C CP-MAS NMR spectra of TiMent-CyPTS-HMDS-MCM-41 reveals, as expected, the presence of the capped agent, triazine silane ligand and isopropoxo ligands bonded to the metal centre, besides a new pattern of signals attributed to the menthoxo unit is observed (see Section 2). As characteristic signals it is worthy to mention the signals of the isopropoxo ligand at 21 and 68 ppm for methyl $(\boldsymbol{C}H_3)_2–CH–O$ and methyne $(CH_3)_2–\boldsymbol{C}H–O$ groups, respectively, the signal corresponding to the aromatic carbons $\boldsymbol{C}_3N_3$ of triazine at 145 ppm, the trimethylsilyl carbon atoms $(\boldsymbol{C}H_3)_3Si–O–Si\equiv$ of the silylating agent at −2.5 ppm and the C1 of the menthoxo unit at 84 ppm.

The TGA curves of the modified material Ti-CyPTS-HMDS-MCM-41 and TiMent-CyPTS-HMDS-MCM-41 are given in Fig. 7. The curves show a small loss in mass when heated until 150 °C, which is interpreted as the loss of physically adsorbed water. For Ti-CyPTS-HMDS-MCM-41 the degradation process occurs in two steps. In the first step, between 185 and 350 °C, the weight loss is due to the break down of pendant triazine propyl groups–titanium alkoxo complexes tethered on the silica surface. Between 425 and 600 °C the weight loss is attributed to the break down of silylating agent. The TGA curve of TiMent-CyPTS-HMDS-MCM-41 shows that an

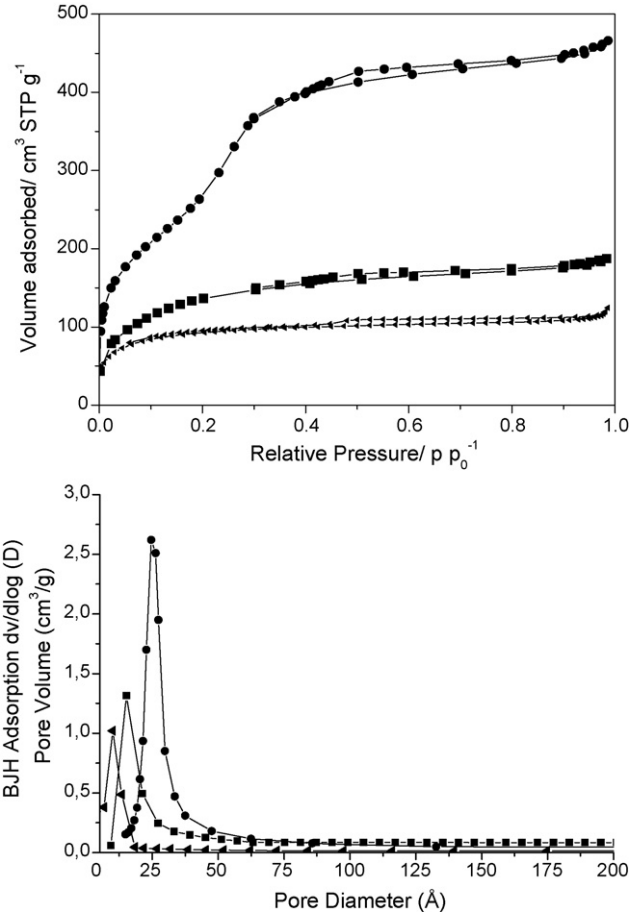

Fig. 2. Nitrogen adsorption–desorption isotherms profiles and pore size distribution of (●) MCM-41, (■) Ti-CyPTS-HMDS-MCM-41 and (◄) TiMent-CyPTS-HMDS-MCM-41.

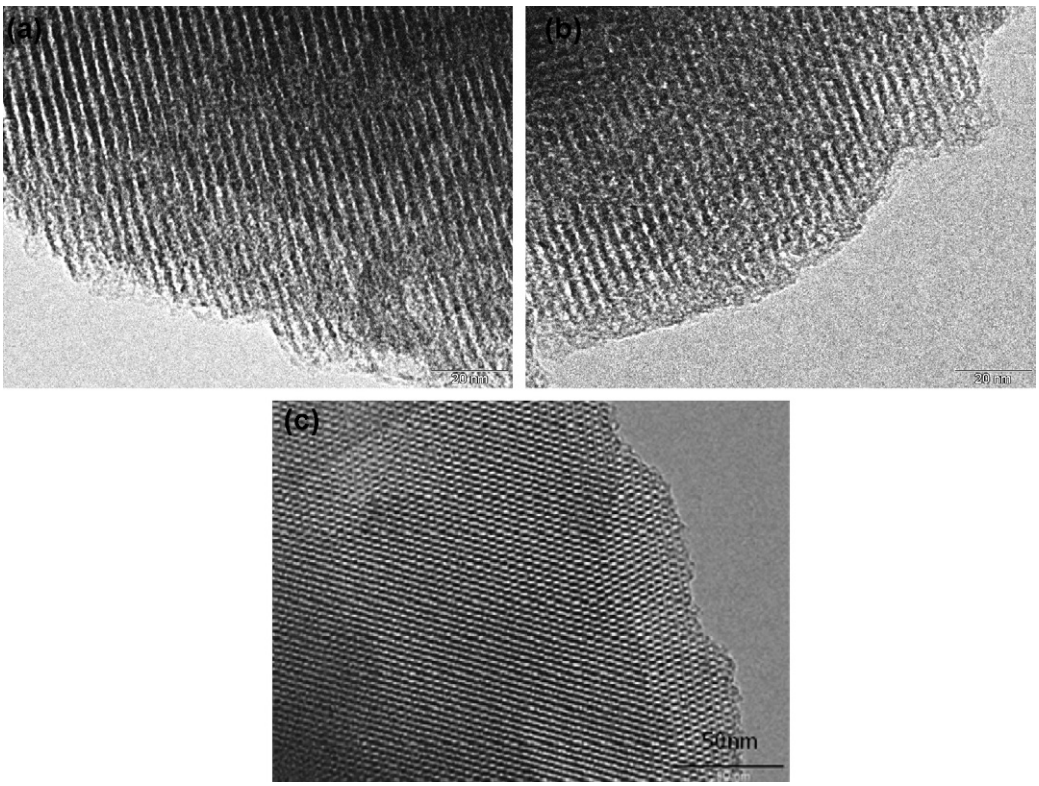

Fig. 3. TEM image of (a) Ti-CyPTS-HMDS-MCM-41, (b) TiMent-CyPTS-HMDS-MCM-41 and (c) Ti(L-DET)-CyPTS-HMDS-MCM-41. The staff rule represented 20 nm, for (a), (b) and 50 nm for (c), respectively.

additional degradation process occurs between 100 and 200 °C, probably due to the break down of the bulky menthoxo ligands in comparison with the former sample. The break down of the titanium isopropoxo moieties tethered on silica surface and the silylating agents take place, as expected, between 200–350 and 350–600 °C, respectively. The thermal stability of these samples is also in agreement with previous results given in the literature for other functionalized mesoporous silicas [27].

3.2. Preparation of Ti(L-DET)-CyPTS-HMDS-MCM-41

To gain insight into the chemistry of the epoxidation process, the solid obtained by reaction of Ti-CyPTS-HMDS-MCM-41 and the chiral tartrate, L-DET, was fully characterized. Important features related to the reaction of the L-DET with the metallic complex immobilized upon MCM-41 can be obtained from ^{13}C MAS NMR in the solid state as shown in Fig. 8. The carbon atom of the carbonyl group in the tartrate ligand appears dishielded at 171 ppm, besides the carbon atom attached to the hydroxyl group appears at 85 ppm.

IR spectra confirmed the modification of the system Ti-CyPTS-HMDS-MCM-41 by reaction with L-(+)-DET. The Ti tartrate-grafted samples exhibited a carbonyl band of tartrate at 1741 cm^{-1} in their spectra (see Fig. 9b), with a very small shifts of their carbonyl bands in comparison with free-(L-DET). The titanium samples did not exhibit the typical carbonyl bands at 1680 cm^{-1} assigned to ester groups bound to titanium through the carbonyl oxygen in the Sharpless system [28]. The TGA curve of this solid shows three peaks for weight loss. The first weight loss (endothermic) below 100 °C

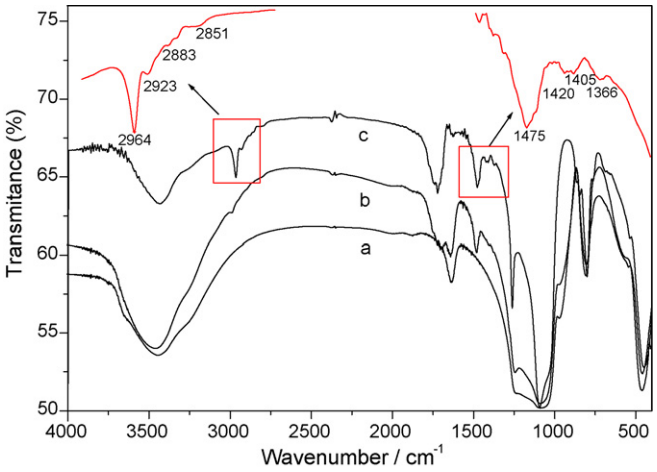

Fig. 4. FT-IR spectra of (a) MCM-41, (b) Ti-CyPTS-HMDS-MCM-41 and (c) TiMent-CyPTS-MTMS-MCM-41.

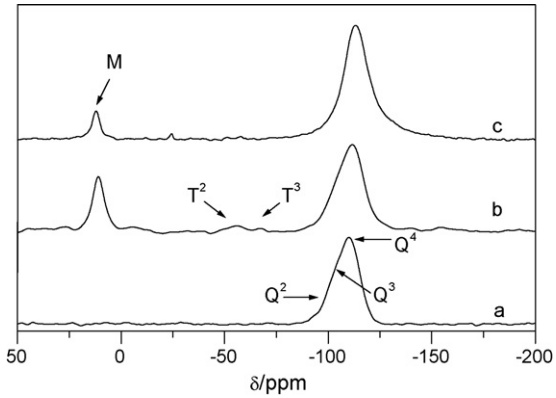

Fig. 5. ^{29}Si MAS NMR results of (a) MCM-41, (b) Ti-CyPTS-HMDS-MCM-41 and (c) TiMent-CyPTS-HMDS-MCM-41.

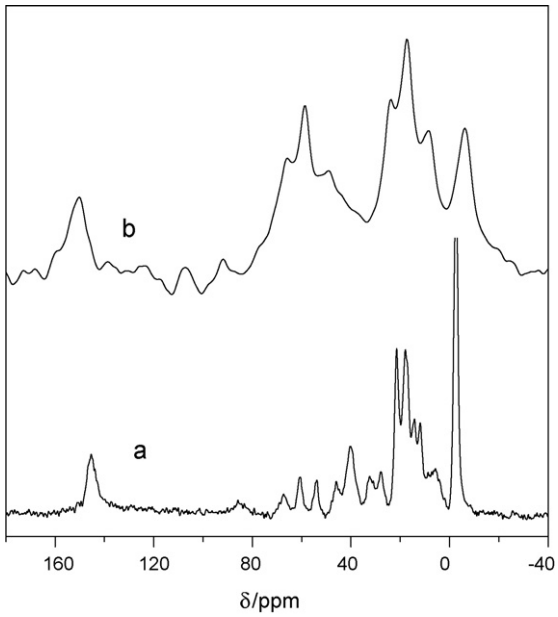

Fig. 6. ^{13}C NMR of (a) TiMent-CyPTS-HMDS-MCM-41 and (b) Ti-CyPTS-HMDS-MCM-41.

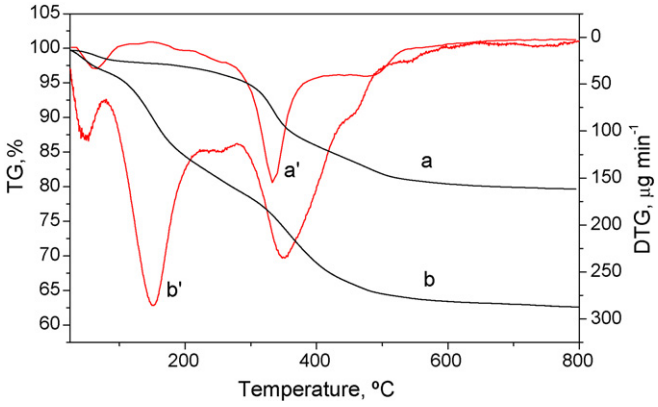

Fig. 7. Thermogravimetric curves for (a) Ti-CyPTS-HMDS-MCM-41 and (b) TiMent-CyPTS-HMDS-MCM-41.

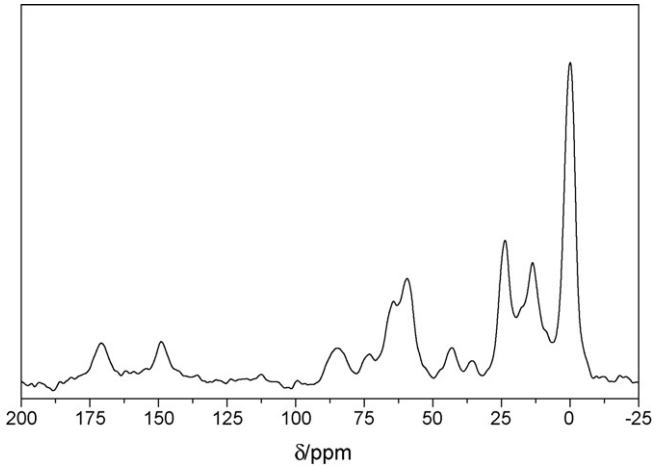

Fig. 8. ^{13}C NMR of Ti-CyPTS-HMDS-MCM-41 after reaction with L-DET.

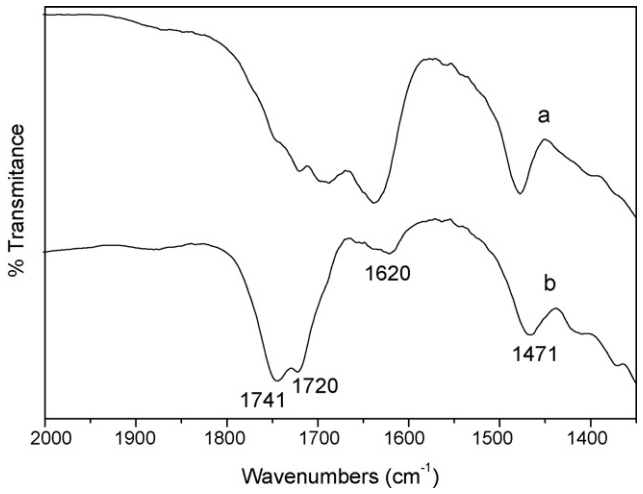

Fig. 9. FT-IR spectra of (a) Ti-CyPTS-HMDS-MCM-41 and (b) Ti-CyPTS-HMDS-MCM-41 + L-(+)-DET in the CO-stretching region.

corresponds to the loss of physisorbed water molecule. For the neat complex Ti-CyPTS-HMDS-MCM-41 there is one weight loss in the range of 185–350 °C, which is shifted to 100–250 °C in the case of Ti(L-DET)-CyPTS-HMDS-MCM-41 (Fig. 10), indicating that the presence of the chiral auxiliar decreases the stability of the solid. The additional third weight loss would correspond to the removal of the titanium isopropoxo moieties tethered on silica surface and the silylating agents.

3.3. The UV–vis/DRS spectra

The diffuse reflectance UV–vis spectra (DRUV–vis) of the samples (see Fig. 11) were essential for a proper understanding of the nature of the metal species, especially supporting and complementing previous characterization data of these materials. The DRUV–vis spectrum of Ti-CyPTS-HMDS-MCM-41 (taken under ambient air conditions) exhibits a strong absorption at λmax = 210 nm for the oxygen to Ti (IV) charge transfer band (LMCT). Absorption maxima in the range of 210–240 nm are attributed to a LMCT for true four-coordinate Ti (IV). Furthermore, a well-defined absorption peak is observed at 280 nm, indicative of the presence of titanium species with higher coordination environments. It seems to be that the chelating triazine ligands may provide a penta-coordinated environment; furthermore, the ligands attached to flexible alkyl chains are near enough to allow some degree of oligomerization between

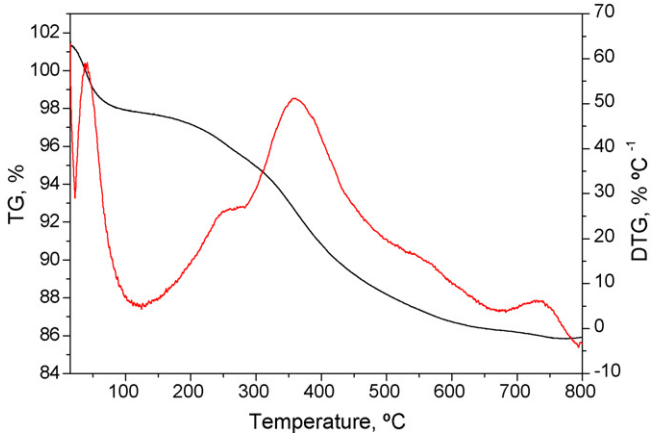

Fig. 10. Thermogravimetric curve for Ti-CyPTS-HMDS-MCM-41 after reaction with L-DET.

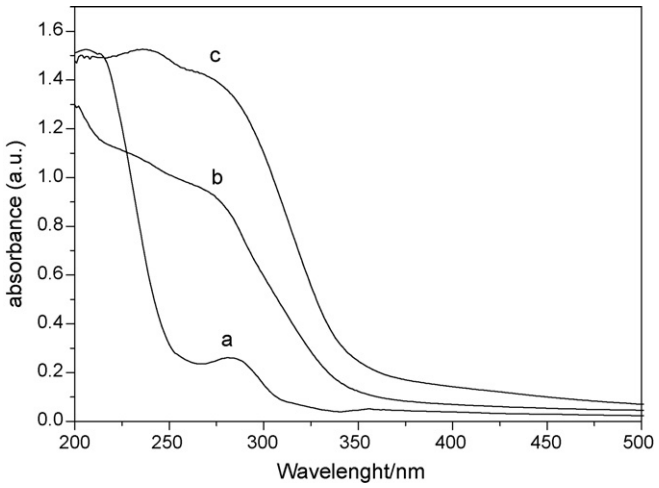

Fig. 11. Solid state diffuse reflectance UV–vis spectra of (a) Ti-CyPTS-HMDS-MCM-41, (b) Ti(L-DET)-CyPTS-HMDS-MCM-41 and (c) TiMent-CyPTS-HMDS-MCM-41.

metallic units given the higher tendency of this metal to saturate its binding sphere. Therefore, it is probable that in some of the titanium complexes on the silica surface the central core consists of an inter-linked titanium isopropoxo moiety as observed frequently for these types of derivatives [29]. Similarly, the DRUV–vis spectrum of TiMent-CyPTS-HMDS-MCM-41, although presents broad signals, contains absorption bands at 209, 240 and 275 nm, indicating the existence of both titanium tetrahedrically coordinated titanium and titanium centres with higher coordination environment provided, as mentioned above, by both the chelating triazine ligand and by certain degree of oligomerization with neighbouring units. The introduction of L-DET acting as a di-coordinated ligand, changes the spectra showing the appearance of a new band typical of tartrate ligand at 237 nm and the band at 272 nm previously observed assigned to hexa-coordinated titanium [30]. The Sharpless mechanism usually accepted requires a coordination sphere in which the four d electrons of titanium are involved in sigma bonds with a tartrate group chelating the metal through two sigma bonded oxygen atoms an allyl alkoxy group and a sigma/pi coordinated tert-butyl peroxo group. In our system, in principle, the tartrate ligand should bond the metal through two sigma bonded oxygen atoms so the activity and selectivity of the reactions may result from a monomeric titanium complex. Nevertheless, the presence of dinuclear species suggested on basis on their DR-UVA–vis spectra (see Fig. 12), similar to those evidenced by other authors must not be discarded [31].

3.4. Catalytic cinnamyl alcohol epoxidation

The chiral catalyst obtained in situ by adding the chiral auxiliary (+)-diethyl-L-tartrate to Ti-CyPTS-HMDS-MCM-41 was tested in the enantioselective epoxidation of cinnamyl alcohol. In addition, TiMent-CyPTS-HMDS-MCM-41 (MentO = 1R,2S,5R-(−)-menthoxo)) was tested, as well. The results presented in Table 3 show that the enantioselectivity of Ti-CyPTS-HMDS-MCM-41 (entry 2) plus L-(+)-ethyl tartrate, as asymmetry inductor, is slightly lower but still comparable to that obtain with the homogeneous system (entry 3), obtaining as expected the (2*S*,3*S*)-epoxide as the major enantiomer. The conversion increases with time (entries 2–6) and is depending on titanium amount. As can be seen when the titanium/substrate ratio increased from 1/20 to 1/10 (entries 2 and 7) the conversion increase significantly, although the obtained values are still low in comparison with the counterpart catalyst in solution. Previously, Li et al. [15] have justified this result as a consequence of the low diffusion of the substrate and the product in the mesopores of MCM-41. On the contrary, TiMent-CyPTS-HMDS-MCM-41 (entry 8), whose asymmetry is based on the menthoxo unit bonded directly to titanium centre, show better yield but poor enantiomeric excess. If menthol is tested as chiral auxiliar and added in situ to Ti-CyPTS-HMDS-MCM-41 (entry 9) the enantioselectivity is nearly doubled, but still far away from those of the tartrate system. The major enantiomer is the (2S,3S)-epoxide, however, the experimental results show that the (2R,3R)-epoxide is obtained as the

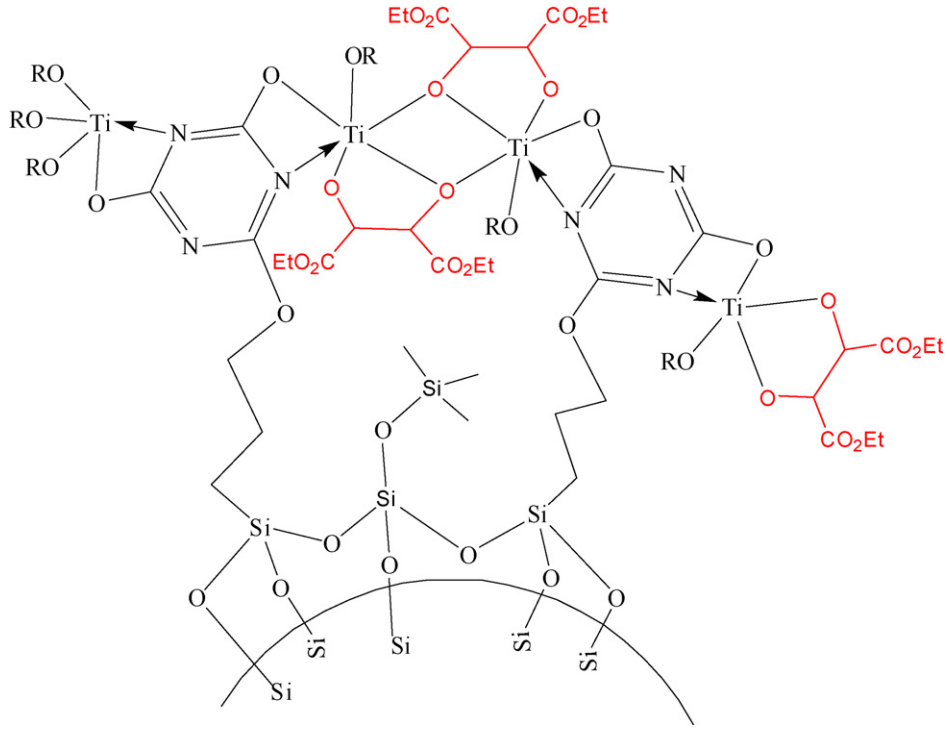

Fig. 12. Proposed structure for titanium complex immobilized onto the silylated MCM-41 surface.

Table 3
Asymmetric epoxidation of cinnamyl alcohol with Ti-CyPTS-HMDS-MCM-41 and TiMent-CyPTS-HMDS-MCM-41.

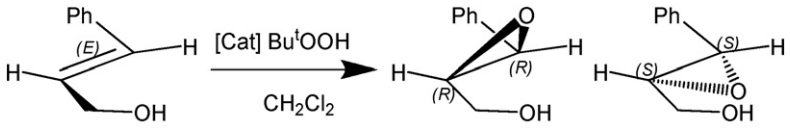

Catalyst	Chiral auxiliar	Molar ratio Ti/BuᵗOOH/substrate/ chiral auxiliar	Reaction time (h)	ee (%)	Configuration	Yield (%)
1. [{Ti(O*i*Pr)$_2$(OMent)}$_2$]	–	1/40/20/0	12	17	2*R*,3*R*	60
2. [{Ti(O*i*Pr)$_3$}$_3$ $C_3N_3O_3$]	L-DET	1/40/20/1.35	12	78.4	2*S*,3*S*	58
3. Ti-CyPTS-HMDS-MCM-41	L-DET	1/40/20/1.35	12	70.6	2*S*,3*S*	9
4. Ti-CyPTS-HMDS-MCM-41	L-DET	1/40/20/1.35	36	76	2*S*,3*S*	10
5. Ti-CyPTS-HMDS-MCM-41	L-DET	1/40/20/1.35	48	65	2*S*,3*S*	21
6. Ti-CyPTS-HMDS-MCM-41	L-DET	1/40/20/1.35	60	68	2*S*,3*S*	50
7. Ti-CyPTS-HMDS-MCM-41	L-DET	1/20/10/1.35	12	81	2*S*,3*S*	24
8. TiMent-CyPTS-HMDS-MCM-41	–	1/40/20/0	12	3	2*S*,3*S*	59
9. Ti-CyPTS-HMDS-MCM-41	1R,2S,5R-(−)-menthol	1/40/20/1.35	36	6.2	2*S*,3*S*	19
10. First recycle experiment Ti-CyPTS-HMDS-MCM-41	L-DET	1/40/20/1.35	36	77	2*S*,3*S*	14

preferred enantiomer when using [{Ti(O*i*Pr)$_2$(OMent)}$_2$] as homogeneous catalyst (entry 1). This change in asymmetry induction originated by the same chiral ligand upon immobilization in the mesoporous of MCM-41 has been previously observed by our group [14]. Inverted enantioselectivity has been observed in our system after immobilization. It is proposed that the confinement in chiral synthesis is essentially a consequence of substrate's interaction with both the pore wall and the chiral directing groups [32,33].

The stabilities of the modified materials were studied by recycling the recovered solids. Before reuse, the solid was separated by filtration from the reaction solution, thoroughly washed with dichloromethane and dried at room temperature. The catalysts were found to be active still after been recovered with similar catalytic activity and enantioselectivity to those obtained in the first run (entry 10). In order to determine whether the active species leached into solution during a typical run, control filtrate experiments were performed. Two samples of the titanium-supported precursor Ti-CyPTS-HMDS-MCM-41 was stirred in dichloromethane at −20 °C during 2 h in the presence of, BuᵗOOH, cinnamyl alcohol and L-DET in 1/20/10/1.35 molar ratio. One of the mixtures was then filtered off and the filtrated was stirred 12 additional hours under similar experimental conditions, after the appropriate work up the filtrate shows a 5% yield and 58% ee, meanwhile the second sample stirred 12 additional hours shows 25% and 81% ee, respectively; indicating that leaching of catalytically active titanium species into solution is negligible.

4. Conclusions

The process that immobilize metallic complexes via covalent linkage between the ligand and the support, using a multistep grafting approach, seems to be a good method to obtain well-defined titanium species, catalytically active in the asymmetric epoxidation of cinammyl alcohol. The heterogenization of titanium complexes caused remarkable changes as the reactivity was concerned. The reaction time was greatly increased upon immobilization what strongly suggests that the reaction took place in the pores where the presence of chiral auxiliar, oxidant and substrate is regulated by the pore size. In fact, due to the confinement effect the asymmetry induction originated by the 1R,2S,5R-(−)-menthoxo ligand was the opposite to that originated by the homogeneous system. Finally, conversion and enantioselectivity remains constant after use from fresh to first recycle over Ti-CyPTS-HMDS-MCM-41. We are currently investigating new catalytic properties of these heterogeneous systems and modification of the ligands and support in our laboratory in order to improve the efficiency of the epoxidation process.

Acknowledgements

We gratefully acknowledge financial support from the CAM (project S-0505/PPQ-0328) and from MICINN (project CTQ2008-05892/BQU).

References

[1] T.P. Yoon, E.N. Jacobsen, Science 299 (2003) 1691.
[2] (a) S. Caron, R.W. Dugger, S.G. Ruggeri, J.A. Ragan, D.H. Brown Ripin, Chem. Rev. 106 (2006) 2943;
(b) V. Farina, J.T. Reeves, C.H. Senanayake, J.J. Song, Chem. Rev. 106 (2006) 2734.
[3] (a) Q.-H. Xia, H.-Q. Ge, C.-P. Ye, Z.-M. Liu, D.-X. Su, Chem. Rev. 105 (2005) 1603;
(b) Choong Eui Song, Dong Hyun Kim, Doo Seoung Choi, Eur. J. Inorg. Chem. (2006) 2927.
[4] N. End, K.-U. Schöning, Top. Curr. Chem. 242 (2004) 241.
[5] (a) R.I. Kureshy, I. Ahmad, N.H. Khan, S.H.R. Abdi, K. Pathak, R.V. Jasra, Tetrahedron: Asymmetry 16 (2005) 3562;
(b) T. Soundiressane, S. Selvakumar, S. Ménage, O. Hamelin, M. Fontecave, Anand P. Singh, J. Mol. Catal. A: Chem. 270 (2007) 132;
(c) Lu-Ning Huang, Xin-Ping Hui, Peng-Fei Xu, J. Mol. Catal. A: Chem. 258 (2006) 216.
[6] K. Aoki, T. Shimada, T. Hayashi, Tetrahedron: Asymmetry 15 (2004) 1771.
[7] H. Yang, J. Li, J. Yang, Z. Liu, Q. Yang, C. Li, Chem. Commun. (2007) 1086.
[8] R.A. García, R. Van Grieken, J. Iglesias, V. Morales, D. Gordillo, Chem. Mater. 20 (2008) 2964.
[9] A. Adima, J. Moreau, M. Wong Chi Man, Chirality 12 (2000) 411.
[10] Choong Eui Song, Annu. Rep. Prog. Chem., Sect. C 101 (2005) 143.
[11] B.M. Choudary, V.L.K. Valli, A. Durga Prasad, J. Chem. Soc., Chem. Commun. (1990) 1186.
[12] M.C. Klunduik, T. Maschmeyer, J.M. Thomas, B.F.G. Johnson, Chem. Eur. J. 5 (1999) 5.
[13] D. Meunier, A. Piechaczyk, A. Mallmann, J.M. Basset, Angew. Chem. Int. Ed. 23 (1999) 38.
[14] Z.-H. Fu, D.-L. Yin, W. Zhao, A.-X. Lv, D.-H. Yin, Y.-Z. Xu, L.-X. Zhang, J. Mol. Catal. A: Chem. 208 (2004) 159.
[15] Y. Pérez, D. Pérez Quintanilla, M. Fajardo, I. Sierra, I. del Hierro, J. Mol. Catal. A: Chem. 271 (2007) 227.
[16] S. Xiang, Y. Zhang, Q. Xin, C. Li, Angew. Chem. Int. Ed. 5 (2002) 41.
[17] R. Ballesteros, Y. Pérez, M. Fajardo, I. Sierra, I. del Hierro, Micropor. Mesopor. Mater. 116 (2008) 452.
[18] Y. Pérez, I. del Hierro, M. Fajardo, A. Otero, J. Organomet. Chem. 679 (2003) 220.
[19] M.V. Landau, S.P. Varkey, M. Herskowitz, O. Regev, S. Pevzner, T. Sen, Z. Luz, Micropor. Mesopor. Mater. 33 (1999) 149.
[20] S. Morante-Zarcero, Y. Pérez, I. del Hierro, M. Fajardo, I. Sierra, J. Chromatogr. A 1046 (2004) 61.
[21] D.J. Ramón, M. Yus, Chem. Rev. 106 (2006) 6.
[22] (a) I. Kuzniarska-Biernacka, A.R. Silva, A.P. Carvalho, J. Pires, C. Freire, J. Mol. Catal. A: Chem. 278 (2007) 82;
(b) F. Bigi, L. Moroni, R. Maggi, G. Sartori, Chem. Commun. (2002) 716.
[23] B. Parker, D.Y. Son, Inorg. Chem. Commun. 5 (2002) 516.
[24] R.L. Brutchey, B.V. Mork, D.J. Sirbuly, P. Yang, T.D. Tilley, J. Mol. Catal. A: Chem. 1 (2005) 238.
[25] J. Jarupatrakorn, D.T. Tilley, J. Am. Chem. Soc. 124 (2002) 8380.

[26] (a) E. Pretsch, T. Clero, J. Seibl, W. Simon, Tablas para la elucidación estructural de compuestos orgánicos por métodos espectroscópicos, Alhambra, Madrid, 1991;
(b) P.G. Lampman, G. Kriz, Introduction to Spectroscopy, Harcourt College Publishers, USA, 2001.
[27] (a) B. Lee, Y. Kim, H. Lee, J. Yi, Micropor. Mesopor. Mater. 50 (2001) 77;
(b) D.J. Macquarrie, D.B. Jackson, J.E.G. Mdoe, H.J. Clark, New J. Chem. 23 (1999) 539;
(c) L. Bois, A. Bonhommé, A. Ribes, B. Pais, G. Raffin, F. Tessier, Colloids Surf. A: Physicochem. Eng. Aspects 221 (2003) 221.
[28] M.G. Finn, K. Barry Sharpless, J. Am. Chem. Soc. 113 (1991) 113.
[29] (a) H. S Fric, M. Puchberger, U. Schubert, Eur. J. Inorg. Chem. (2008) 1452;
(b) S.D. Nogai, O. Schuster, J. Bruce, H.G. Raubenheimer, New J. Chem. 32 (2008) 540.
[30] (a) F. Chiker, F. Launay, J.P. Nogier, J.L. Bonardet, Green Chem. 5 (2003) 318;
(b) E. Gianotti, A. Frache, S. Coluccia, J.M. Thomas, T. Maschmeyer, L. Marchese, J. Mol. Catal A: Chem. 483 (2003) 204.
[31] A.O. Bouth, G.L. rice, S.L. Scott, J. Am. Chem. Soc. 121 (1999) 7201.
[32] A. Corma, A. Fuerte, M. Iglesias, F. Sanchez, J. Mol. Catal. A: Chem. 107 (1996) 225.
[33] B.F.G. Johnson, S.A. Raynor, D.S. Shephard, T. Mashmeyer, J.M. Thomas, G. Sankar, S. Bromley, R. Oldroyd, L. Gladden, M.D. Mantle, Chem. Commun. (1999) 1167.